This is a peer-reviewed, author's accepted manuscript of the following research article: Farooqui, T. A., Belwanshi, V., Rane, K., Bhole, K. S., & Oak, S. (2022). Numerical analysis of joule heating in a Ni–Ti segmented wire used in sensing applications. *Journal of The Institution of Engineers (India): Series D*. https://doi.org/10.1007/s40033-022-00392-4

Numerical Analysis of Joule Heating in a NiTi Segmented Wire used in Sensing Applications

Tareq Ahmed Farooqui[1*], Vinod Belwanshi[2], Kedarnath Rane[3], Kiran Bhole[1], Sachin Oak[1]

[1]Department of Mechanical Engineering, Sardar Patel College of Engineering, Andheri, Mumbai, India, 400058

[2]School of Physics and Astronomy, College of Science and Engineering, University of Glasgow, Glasgow, UK G12 8QQ

[3]National Manufacturing Institute Scotland, 85 Inchinnan Dr, Inchinnan Renfrew, Scotland, PA4 9LJ

*Corresponding author Email: tareqahmedf@gmail.com

Abstract

Use of shape memory alloy (SMA) has been extensively increased to fabricate sensors and actuators. It is because of its inherently unique properties such as pseudo-elasticity and shape memory effect (SME). Among various SMA's, Ni-Ti SMA has received a prime interest in various applications. However, Ni-Ti SMA based sensors suffer from the Joule heating effect as their performance is impacted due to an increase in the temperature. This work presents a finite element analysis (FEA) approach to estimate a rise in temperature in Ni-Ti SMA sensors. A numerical model was developed in COMSOL, considering a Ni-Ti with Cu segment. Electro-thermal boundary conditions were set to assess the thermal response of the segmented wire. Multiple simulation runs were carried out by varying material and geometric characteristics of segmented wire. The results are validated against the literature and quantitative estimation of thermal characteristics through physics driven analytical model. Simulation results show that the Joule heating effect has a significant effect on the properties of the material which can be considered while designing and selecting the sensor application. This study further brought a few mitigation actions which can minimize the Joule heating effect without hindering the performance of Ni-Ti SMA based sensors.

Keywords: *Ni-Ti; SMA; Joule-heating; Segmented wire; Finite element analysis.*

1. Introduction

Over the last few decades, shape memory alloys (SMAs) have gained traction in a number of industries, including biomedical, mechanical, aerospace, and automotive [1-3] because of its features like as pseudo-elasticity and shape memory (SME). These characteristics, together with its ductility, have allowed Ni-Ti thin wires to be used as active elements in shape memory actuators and sensors [4-6]. SMA based micro heating devices pique the interest of the scientific community since they offer a diverse set of applications and benefits such as gas sensors, flow sensors and humidity sensors [7-10]. SMA micro wire are also used as displacement sensors as it has big response characteristics in terms of deformation to input signal from measurand [11]. SMA based strain sensor works on the principle of electrical conductance and its dependence on the conductor's geometry.

Many researchers have examined the Joule heating effect in micro sensors and actuators. Ahmad et al. [11] described the impact of Joule heating and temperature-dependent zeta potential on electroosmotic flow rate in calorimetric flow sensors. Similarly, Casati et al. [12] studied how different electrical impulses affected the functional fatigue of Ni-Ti micro-wires used in shape memory actuators. Zou-Qing et al. [13] modified couple stress theory and two-variable approach to explore the effect of electro-thermo-mechanical loadings on static bending of three-layered cantilever mirco-beams for analysing expression of tip deflection. S.M. Jaureguizahar et al. [14] designed an experimental method for determining the fatigue life of stress-induced commercial NiTi wire. Experimental method depicted a virtual dog-boned specimen to evaluate the true structural fatigue. Study [14] also discussed the effects of heat on the stress-induced martensitic transformation and its effect on critical stresses.

Soroush Parvizi et al. [15] reviewed the data on how several characteristics such as grain size, morphology, and the addition of other alloying materials such as Copper, Magnesium, and Aluminium. The effect on the properties of Ni-Ti alloys manufactured via powder metallurgy and additive manufacturing methods is exhaustively discussed in the study [15]. The study also presents the effect of inclusion of alloying constituents on properties like shape memory effect (SME), corrosive resistance and transformation temperatures. The functional relationship between the alloying constituents and smart material properties are presented in the study [15]. According to Xiebin Wang et al., [16] selective laser melting (SLM) is proposed as promising technique to control Ni/Ti ratio of Ni-Ti shape memory alloy. This technique gives better control on metallurgical aspects of Ni-Ti resulting in alteration of its mechanical properties and

transformation behaviours. Various samples were created using the SLM technique, with varied process parameters such as scanning speed, hatching distance, and laser power. Study [16] concluded that on changes in scanning speed, hatching distance and laser power, martensite transformation temperature changes owing to Ni loss under various SLM process settings. Researchers [16] also discovered that despite of the considerable range of SLM process settings and the presence of substantial flaws, good mechanical (total elongation > 10%) and functional qualities under tensile mode were attained.

Swadhin Kumar Patel et al. [17] reviewed that SME in SMAs is the conversion of martensitic phase to austenitic phase of Ni-Ti alloys. The chemical composition of austenite and martensite phases is Ni-Ti. Other phases, such as Ni4Ti3 and Ti2Ni, are responsible for the precipitation strengthening and hardness of the material. They also emphasised the benefits of the liquid metallurgical approach for the manufacture of Ni-TIi wire for usage in medical applications. Xiaohua Jiang et al. [18] experimented with Ni-Ti plates for improving its transformation behaviours. Compositionally graded TiNi/NiTi laminates were made by diffusion annealing and successive aging to find widening of transformation temperatures window. Gen Satoh et al. [19] studied the effects of various heat treatment temperatures and time on the mechanical as well as shape memory properties of amorphous, Ti-rich Ni-Ti films bonded on silicon substrates. S. Abbas Raza et al. [20] found in experimentation that equiatomic Ni-Ti alloy composites synthesized by reinforcing Zirconium Oxide possess improvement in shape memory effects. Further, Ni-Ti pre-alloyed powder exhibits increased hardness. Wayman et al. [21] reviewed shape memory alloys from point of view of crystallography of martensitic transformations. Shape memory effect has been universally correlated with a martensitic transformation which is thermoelastic in nature. However, this study [21] focuses on the development of strain due to cyclic loading and other structural parameters.

Despite all the previous studies done on the sensors all of them focuses on the strain and induced stress in the sensor on application of external loading conditions. A few studies have been carried out for the temperature rise due to induction of current into the SMA and the sensor structure. This work represents a simple model for analysing the effect of Joule heating, temperature rise and the percentage of strain developed due to applied current in the sensor. The segmented wire characteristics (the relationship between temperature rise and electric current) was analysed with the change in segmented wire ratio. A potential difference was induced in the segmented wire points so that an electric field is created which leads to Joule heating effect in the conductor. Thermophysical properties (thermal conductivity, density,

coefficient of thermal expansion, specific heat capacity) were induced in the model. Also, wire characteristics were evaluated at different applied electrical potentials. The simulation results show a significant change in characteristics of segmented wire and thus should be considered to decide the key parameters and properties of material while designing the Ni-Ti strain sensor and actuators.

2. Theory and Central Theme of Ni-Ti based Sensor

To analyse the impact of electric-induced Joule heating that dissipates heat due to conduction and convection, the required multi-physics modules are discussed in the current section. It includes solving partial differential equations that govern electric field distribution, solid mechanics, and heat transfer using a modelled segmented wire.

2.1 Electric Field: Electric field is used to compute the distributions of current and potential in conducting media. It solves an Ohm's law-based current conservation equation (Eq. 1) with the scalar electric potential as the dependent variable.

$$\nabla . J = Q_{j.v} \tag{1}$$

The electric field E (V/m) along the segmented wire is not equally distributed and should be computed using Eq. 2

$$J = \sigma E + J_e \tag{2}$$

The stationary electric current was then calculated using the stationary continuity equation (refer Eq. 3), assuming no inductive effects.

$$E = -\nabla V \tag{3}$$

where J is the electric current density (A/m^2), where V is the electric potential, $Q_{j.v}$ is the rate of change of charge density and σ is the temperature-dependent electrical conductivity of the liquid (S/m).

2.2 Heat transfer: Convection is the primary mode of heat transfer from the wire. This heat loss is highly influenced by the wire's excess temperature, the materials physical qualities, and its geometrical design. The differential form of Fourier's law relates to the temperature equation expressed in solid domains (refer Eq. 4).

$$\rho C_p \mathbf{u} \cdot \nabla \mathrm{T} + \nabla \cdot \mathbf{q} = \mathbf{Q} + \boldsymbol{Q_{ted}} \tag{4}$$

Where, ρ is the temperature reliant density in kg/m^3, C_p is the temperature reliant specific heat at constant pressure in J/kg K, ∇T is the temperature gradient in K, Q is the heat transfer and Q_{ted} is the heat generation per unit volume in W/m^3.

Equation (5) is used to calculate the heat generated by the potential difference induced in the wire, which leads to Joule heating.

$$\mathbf{q} = -k\nabla T \tag{5}$$

2.3 Solid Mechanics: In this interface the model external boundary conditions are assigned. The segmented wire is fixed at both its end acting as a fixed beam (refer Figure 1). The detailed geometrical consideration is given in section 3.3.

3. Methodology and materials

3.1 Geometry: The considered segmented wire has the radius 50 µm and length of 6 mm. The Ni-Ti wire is located in the middle of two copper wires as shown in Figure 1. The segmented length ratio (α_{seg}) i.e. ratio of Ni-Ti wire to Cu wire was varied to obtain various change in thermal responses of wire. The segmented wire is assumed to be in room temperature under atmospheric pressure (Figure 1).

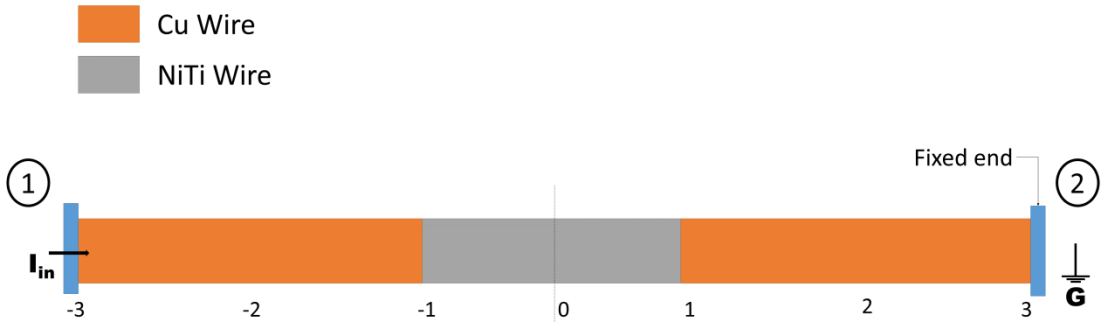

Figure 1: Schematic layout of the segmented micro Ni-Ti wire

3.2 Material: To model the Joule heating effect on the segmented Ni-Ti wire, the copper at the two extreme ends were used. SMA was generally placed in the middle of the segmented wire and it was change according to the segmented wire ratio (α_{seg}) to obtain various simulation results with the change in parameters. The material properties used for the simulation are summarized in Table 1.

Table 1: Thermo-physical properties of Ni-Ti and Cu

Properties	**Ni-Ti**	**Cu**
Thermal conductivity (W/(m-K))	10	385
Coefficient of thermal expansion (1/K)	1.1E-5	16E-6
Heat capacity at constant pressure (J/(kg-K))	320	0.385E-3
Density (kg/m^3)	6450	7764
Relative permittivity	1	1
Electrical conductivity (S/m)	1320000	56
Young's modulus (pa)	70E9	110E9
Poisson's ratio	0.3	0.3

3.3 Boundary conditions:

The boundary conditions applied on the segmented wire model are summarised in Table 2.

Table 2: Boundary conditions for Ni-Ti segmented wire

Field Boundary	Electric current	Heat Transfer	Solid Mechanics
1, 2	Potential [5-25] mA, Ground [0]	Temperature [$T=T_0$]	Fixed constrained
overall	Electrical insulation [n.J=0]	Thermal insulation [-n.q=0]	Not applicable

3.4 Design of Experiment and Parametric Analysis:

Full factorial design of experiment with input consideration of geometry and electric field and its various levels is carried out in design of experiment. Some key parameter like segmented length ratio (α_{seg}), diameter of wire (ϕ) and Current (I) mA are identified. As discussed, segmented length ratio shows change in thermal behavior, hence three levels of each parameter are considered.

Segmented ratio (α_{seg}) is a ratio of length of Ni-Ti wire to length of Cu wire which was varied as 0.2, 0.5,1. The diameter (ϕ) of the wire was varied from 0.12 cm, 0.16 cm and 0.2 cm to find the change in temperature of the wire which helps to analyse its effect on thermos-

electrical behaviour of the wire. The applied electrical potential, and hence current flow in the wire was considered to find the maximum temperature across the wire which was varied as 5 mA, 15 mA and 25 mA. These all parameters are listed in Table 3.

Table 3: Parameters for Design of Experiments applied in Characterization of Ni-Ti

Design parameters	Values		
Segmented Ratio (α_{seg})	0.2	0.5	1
Diameter (ϕ) cm	0.12	0.16	0.2
Current (I) mA	5	15	25

DOE Experiments: For full factorial design of experiment considering all combination of levels (L) and K factors (K) , number of experiments can be calculated by the formula: $N = L^K$

Here L = 3, K = 3; Hence, $N= 3^3= 27$.

For DOE it is required to perform 27 simulations. This results in obtaining the maximum temperature along the Ni-Ti and Cu segment. Maximum change in strain along each segment was also determined.

3.5 Numerical scheme:

The segmented Ni-Ti wire was modelled using COMSOL multi-physics. The COMSOL multi-physics interface was used to simulate Joule heating effect and thermal expansion. The interface consists of three modules i.e. solid mechanics, solid heat transfer, and electric current. The maximum temperature, strain along the wire, electric potential, and isothermal contours in the wire were all determined using these three variables. The parametric sweep feature in stationary study allows the model to be solved for different current inputs and the change in geometry of the model to determine the results. The multi-physics coupling of thermal expansion and electromagnetic heating is used in the stationary study. For the model to produce more accurate results, a physics-controlled mesh with fine grain size was used.

4. Results and discussion

4.1 Electrical Potential:

The distribution of electrical potential across the segmented Ni-Ti wire is shown in Figure 2, for a segmented length ratio of 0.5 and a varying current input as mentioned in Table 3. Electrical potential in Ni-Ti wire is the work done for moving the positive electric charge against the electrical field which is stored in the form of energy. For the segmented wire, the electrical potential increases along the Cu segment of the wire and remains constant along the Ni-Ti segment. Further, it increases again later section of the Cu segment of the wire. This is due to the high electrical resistance of copper than that of Ni-Ti. Thus, there is a temperature rise in the Cu section of the segmented wire resulting in Joule heating effect. The observation shows that for a higher current input, the temperature dependence on electrical potential increases correspondingly. For initial current input of 5 mA, the potential difference obtained was around 3V. Similarly, the experimental study obtained presents that the electrical potential is around 16 V when the current input is increased from 5 mA to 25 mA. Further it is observed that the temperature variation has no effect on the potential difference across the wire. The electric potential across the Ni-Ti segment is constant along its length and varies only in the Cu segment.

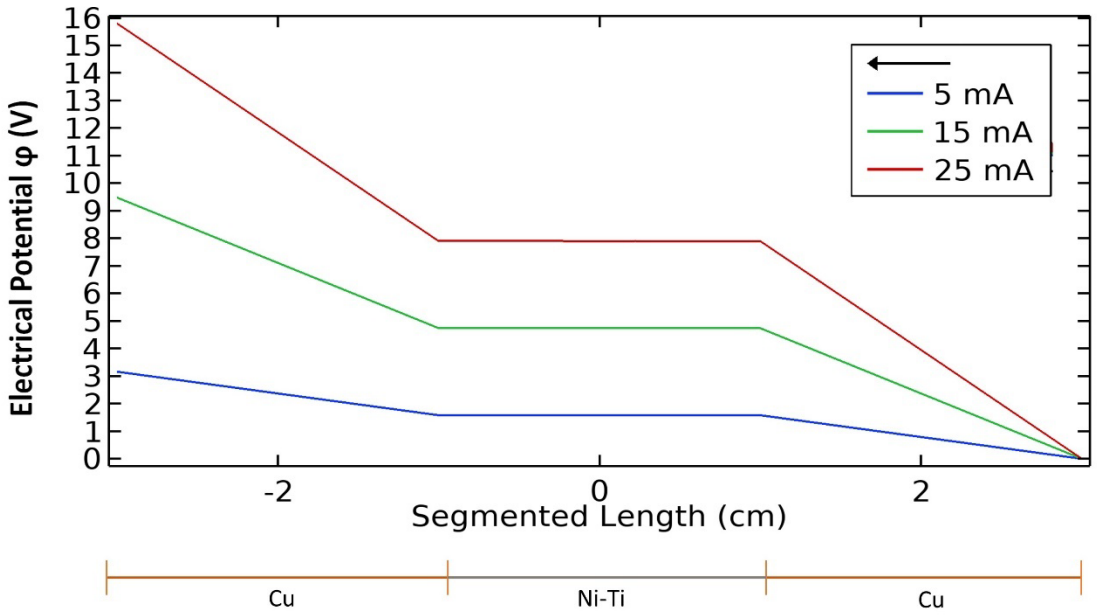

Figure 2: Electric Potential distribution along the Ni-Ti segmented wire for varying current input (red curve= 25 mA, green curve = 15 mA and blue curve= 5 mA) and α_{seg} =0.5.

4.2 Temperature distribution:

Measuring the maximum temperature across the segmented wire using the Joule heating principle is dependent on the applied current in the wire and the resistance provided by the material. Figure 3 depicts the temperature distribution along the segmented wire for each of the segmented length ratios 0.2, 0.5, and 1. The maximum temperature generated along the wire can be seen along the Ni-Ti segment. The simulation results are presented in Figure 3 (a), (b) and (c) for the segmented wire of Ni-Ti. From the simulation it is observed that maximum temperature is obtained in Figure 3 (a) for segmented length ratio equals to 0.2 or alternatively for segmented length as 1 mm. This is because of the presence of copper material in the segment. Figure 3 (b) shows the simulation results for segmented length ratio 0.5 or alternatively for the Ni-Ti segment length of 2 mm. This segment has lesser regime of copper material thus reduces the overall temperature in the segmented wire (refer Figure 3 (b)). Figure 3 (c) shows the simulation results for segmented length ratio 1 or alternaively for the Ni-Ti segmented length of 3 mm. This segment consists of proportional change in copper with the length of the wire. This resulted in comparatively reduced temprerature (22^0C for the similar cases considered in Figure 3 (a) and (b)). For better analysis of the temperature distribution along the segmented wire a spatial distribution of temperaure is drawn for all the segmented ratios. The temperature distribution shown in Figure 3 (a), (b) and (c) presents the rise in temperature for varying current input. According to estimation from Fourier's law of heat conduction, the maximum temperature obtained for a segmented length ratio of 0.2 and a diameter of 0.12 cm is the highest. As the electrical conductivity of Ni-Ti is greater than that of Cu, the temperature along the Ni-Ti segment remains constant and it rises in Cu segment of wire.

Separate simulation results were obtained for the Ni-Ti wire segment to determine strain, temperature rise, and electric potential along the micro wire. Figure 4 depicts a cross-sectional view of the Ni-Ti segment for various output results. The temperature rise was about 22 °C for an input current of 15 mA along the Ni-Ti segment of diameter 0.12 cm and segmented ratio of 0.5, due to the resistivity of Ni-Ti. It is observed that the strain developed is generally at the end points of the wire along the fixed constrained. The Ni-Ti segment swells at the end point due to strain development as current is induced in it and there is a temperature rise along the surface of wire. The electrical potential distribution along the Ni-Ti segment decreases from start point to end point with an average value of 4.74 V.

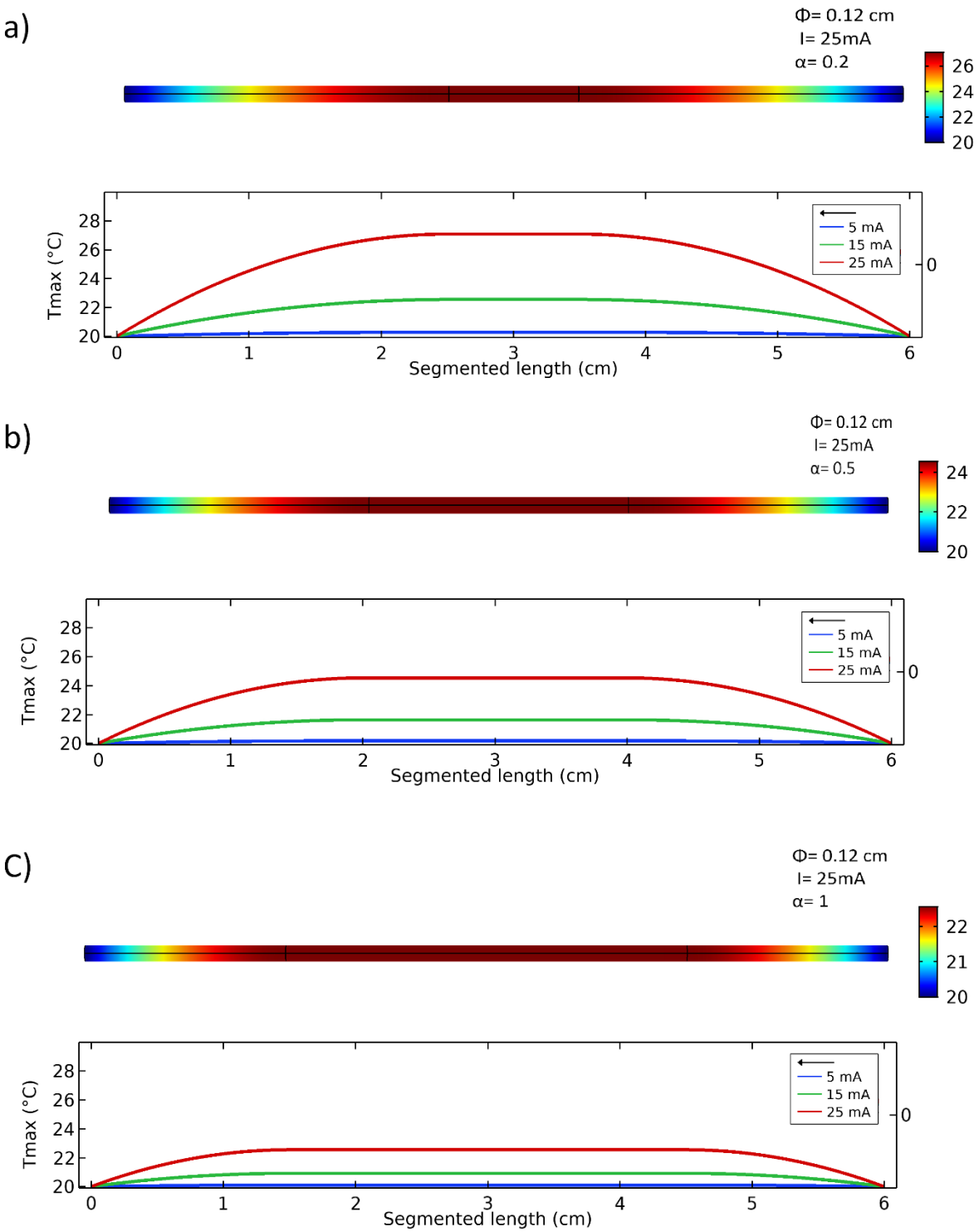

Figure 3: Temperature distribution along the Ni-Ti segmented wire for the diameter of 0.12 cm with varying segmented wire ratio: (a) α=0.2, (b) α=0.5, (c) α=1 with current: I =5mA, 15mA, 25 mA respectively.

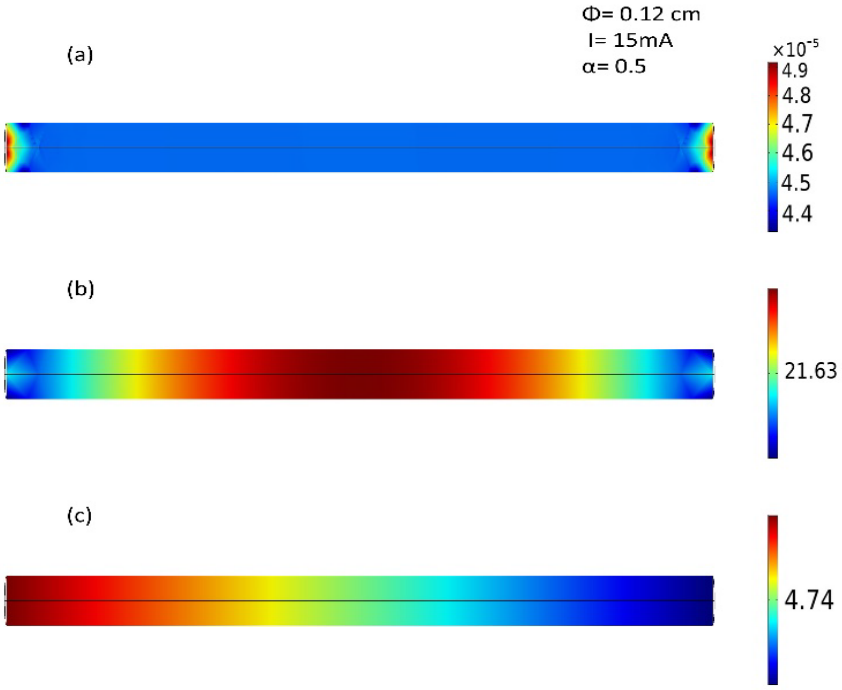

Figure 4: (a) Strain along the Ni-Ti segment for diameter of 0.12 cm and the segment ratio of 0.5. (b) Maximum temperature along the Ni-Ti segment (c) Electric potential along the Ni-Ti segment at the current input of 15 mA.

4.3 Effect of geometrical and electrical parameters on thermal characteristics of segmented wire:

DOE was performed to determine the maximum temperature (T_{max}) rise and strain (ϵ) develop across the segmented wire for various parametric inputs. The simulation's experimental results were also examined. Results in Figure 5 shows that the temperature is rise after changing the parameters such as segmented ratio diameter and current along the wire. The temperature rise in the segmented wire is seen to be primarily caused by the applied potential across the wire.

The diameter and segmented ratio are not as important for smaller potential differences, but when the potential difference is increased to 25 mA, there is a rise in temperature.

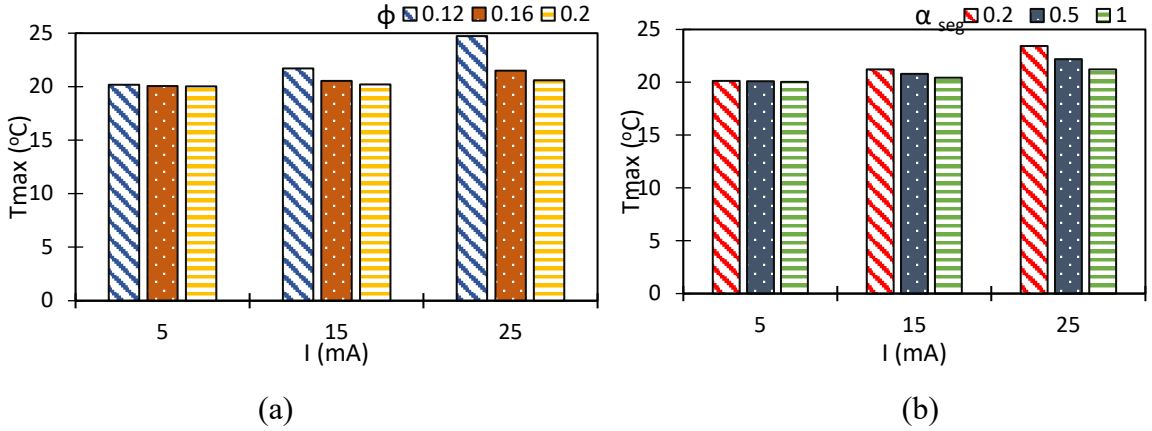

Figure 5: (a) Maximum Temperature vs of electric current with respect to segmented wire ratio (b) Maximum Temperature vs electric current with respect to diameter of wire.

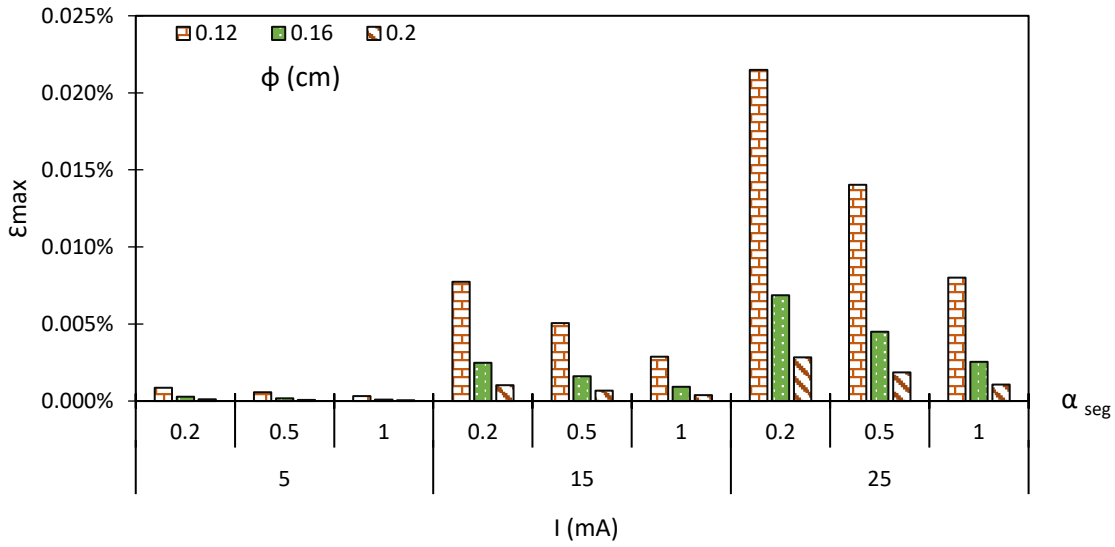

Figure 6: Strain percentage as a function of current and segmented length ratio

The proportion of strain created along the segmented wire was also assessed while varying the diameter, segmented length ratio, and current. Figure 6 shows the percentage of strain obtained. The results show that for the smallest amount of current along the wire, the strain developed is negligible, but as the current input along the wire increases, the strain increases. In comparison to other parameters, the strain percentage obtained for a smaller segmented ratio, i.e. 0.2 with a diameter of 0.12 cm, is comparatively high (0.02 and 0.002 % respectively) (refer Figure 6). The strain generated due to 5 mA potential difference is negligible hence no compensation for strain sensor is required for the model. But for increase in the current input to the segmented wire rise in strain due to swelling of Ni-Ti wire for an increase in current and temperature

respectively is observed. This strain generated need to be compensated for the accurate strain calculation for strain sensor.

4.4 Validation through analytical modeling:

Analytical results of the Ni-Ti segment with a diameter of 0.2 cm and a length of 3 cm for varying current inputs are obtained and used to validate the numerical simulation results for the maximum temperature. The results were obtained by solving the following equations, $Q = I^2R$ followed by resistance $R = \rho L/A$. The heat generated was then calculated by the equation $q_g = Q/AL$ .The wall temperature and the maximum temperature was obtained from the equations (6) and (7).

$$T_W = T_a + \frac{q_g r_o}{2h} \tag{6}$$

$$T_{max} = T_w + \frac{q_g r_o^2}{4k} \tag{7}$$

Analytical and numerical data agree well in the results, implying the accuracy of the proposed analytical model (refer Figure 7). The temperature discrepancy between analytical and numerical calculations is related to the 1D and 3D equations solved analytically. The presented analytical method for Joule heating effect validates proposed model to estimate the temperature generated along the surface.

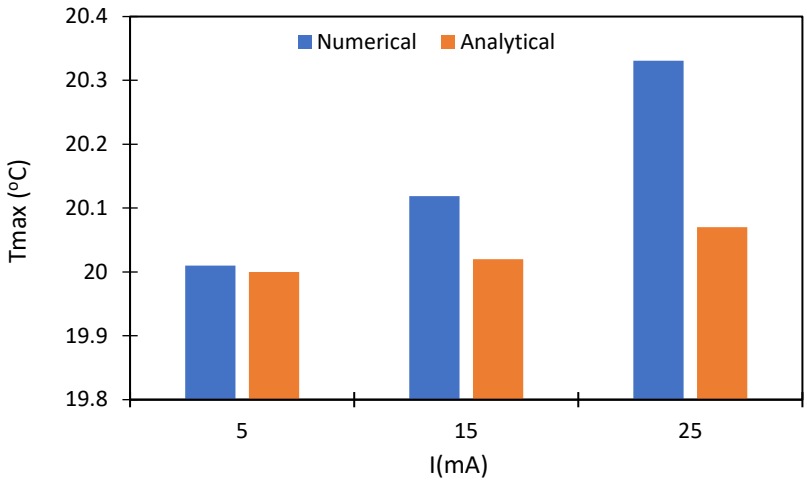

Figure 7: Maximum temperature obtained through analytical and numerical simulations

5. Conclusion

Despite the fact that the use of microsensors has increased intensely in recent decades, there has been limited accurate thermomechanical analysis of microsensors. This paper presents a technique to estimate and simulate the effect of Joule heating in Ni-Ti which is one of the promising microsensor materials. Increase in potential difference along the Ni-Ti segmented wire for varying segmented ratios depicts the actual flow of electrons in the segmented wire. The potential difference generally rises in the Cu segment of the wire due to electrical conductance. Study also discusses the temperature distribution along the segmented wire showing the rise in temperature with respect to the increase in current input. Simulation study shows the temperature rise along the segmented wire in the regime of the Cu segment and remains constant along the Ni-Ti segment. An analytical model was used to validate the numerical study presented. The model depicting temperature distribution is deployed to forecast the strain that would develop along the wire. Joule heating effect caused by the applied current in the segmented wire has a significant influence on the strain developed along the wire. The experimental study shows the linear increase in temperature and strain along the wire as the current is increased from 5 mA to 25 mA. Temperature variations cause the Ni-Ti wire to expand, increasing strain with higher current for a smaller wire segment ratio (0.2). Overall this study presents the guidelines in designing Ni-Ti based sensors to avoid undesirable strain due to Joule heating and points towards provision of the thermal compensation while deploying similar SMA based sensor.

Competing Interests: No potential conflict of interest was reported by the author(s).

Nomenclature

E = electric field, (V/m)

J = electric current density, (A/m^2)

Je = external Current Density

$Q = \text{heat transfer}, J/s$

Q_{ted} = heat generation per unit volume, (W/m^3).

V = electric potential, v

σ = temperature-dependent electrical conductivity, (S/m).

$\nabla T = \text{temperature gradient}$

C_p = temperature-dependent specific heat at constant pressure (J/kg K)

q = local hat flux density

K = thermal of conductivity materials, W/(m-K)

α_{seg} = segmented length ratio

ϕ = diameter of wire, mm

I = current, mA

T_{max} = maximum temperature, °C

ε_{max} = maximum strain

Φ = electric potential, V

References

[1] V. Humbeck J, Non-medical applications of shape memory alloys. Materials science and Engineering, vol 273–275, pp. 134-148, (1999).

[2] Duerig T, Pelton A, Stöckel D, An overview of Ni-Tinol medical applications. Materials Science and Engineering, vol 273–275, pp. 149-160, (1999).

[3] Biscarini A, Mazzolai G, Tuissi A, Enhanced Ni-Tinol properties for biomedical applications, Recent patents on biomedical engineering, vol 1, pp. 180-196(17) (2008).

[4] Nespoli A, Besseghini S, Pittaccio S, Villa E, Viscuso S, The high potential of shape memory alloys in developing miniature mechanical devices: A review on shape memory alloy mini-actuators, Sensors and Actuators, vol 158, pp. 149-160 (2010).

[5] Kohl M, Skrobanek K D, Linear microactuators based on the shape memory effect, Sensors and Actuators, Proceedings of International Solid State Sensors and Actuators Conference, vol 2, pp. 785-788, (1997).

[6] Balakrishnan, V., Phan, H.-P., Dinh, T., Dao, D. V., and Nguyen, N.-T., Thermal Flow Sensors for Harsh Environments, Sensors, 17(9), pp. 2061, (2017).

[7] Dibbern U, A Substrate for Thin-Film Gas Sensors in Microelectronic Technology, Sens. Actuators B, 2(1), pp. 63–70, (1990).

[8] Hung, S.-T,Wong, S.-C., and Fang, W., The Development and Application of Microthermal Sensors With a Mesh-Membrane Supporting Structure, Sens. Actuators A, 84(1), pp. 70-75, (2000).

[9] Dai, C.-L., A Capacitive Humidity Sensor Integrated With Micro Heater and Ring Oscillator Circuit Fabricated by CMOS–MEMS Technique, Sens. Actuators B, 122(2), pp. 375-380, (2007).

[10] S. H. Nahm, Y. I. Kim, J. M. Kim. A Study on the Application of Ni-Ti Shape Memory Alloy as a Sensor, Materials Science Forum Vol 475-479), pp.2043-2046, (2005).

[11] Ahmad A, Yu S, Mohamed A, Effect of Joule heating and temperature-dependent zeta potential on electroosmotic flow measurements in calorimetric flow sensors, IET, Vol 14(9), pp.1007-1012, (2019).

[12] R. Casati, F. Passaretti, A. Tuissi, Effect of electrical heating conditions on functional fatigue of thin Ni-Ti wire for shape memory actuators, Procedia Engineering, vol 10, pp.3423–3428, (2011).

[13] Zou-Qing Tan, Yang-Chun Chen, Size-dependent electro-thermo-mechanical analysis of multilayer cantilever microactuators by Joule heating using the modified couple stress theory, Composites Part B vol 161, pp183–189, (2019).

[14] S.M. Jaureguizahar, M.D. Chapetti, A. Yawny, A novel experimental method for assessment of intrinsic functional and structural fatigue of pseudoelastic NiTi wires, International Journal of Fatigue vol 116, pp 300-305, (2018).

[15] Soroush Parvizi, Seyed Mahdi Hashemi, Fatemeh Asgariniaa,Mohammadreza Nematollahib, Mohammad Elahinia, Effective parameters on the final properties of NiTi-based alloys manufactured by powder metallurgy methods: A review, Progress in Materials Science vol 117, pp.100739. (2021).

[16] Xiebin Wanga, Jingya Yua, Jiangwei Liub, Liugang Chenc, Qin Yangd, Huiliang Weie, Jie Sunb, Zuocheng Wanga, Zhihui Zhangf, Guoqun Zhaoa, Jan Van Humbeeckc, Effect of process parameters on the phase transformation behavior and tensile properties of NiTi shape memory alloys fabricated by selective laser melting, Additive Manufacturing, vol 36, pp.101545, (2020).

[17] Swadhin Kumar Patel, Biswajit Swain, Rakesh Roshan, Niroj K. Sahu, A. Behera, A brief review of shape memory effects and fabrication processes of NiTi shape memory alloys, Materials Today: Proceedings, vol 33(8), pp 5552-5556,(2020).

[18] Xiaohua Jiang, Daqiang Jiang, Yanjun Zheng, Lishan Cui, Transformation behavior of explosively welded TiNi/TiNi laminate after diffusion annealing and aging, Materials Research Bulletin, vol 48 (12), pp.5033-5035, (2013).

[19] Gen Satoh, Andrew Birnbaum, and Y. Lawrence Yao, Effect of annealing parameters on the shape memory properties of NiTi thin films, ICALEO ,p.126 (2008).

[20] S. Abbas Raza, M. Imran Khan, M. Ramzan Abdul Karim, Rashid Ali, M. Umair Naseer, S. Zameer Abbas, Mairaj Ahmad, Effect of Zirconium Oxide Reinforcement on Microstructural, Electrochemical, and Mechanical Properties of TiNi Alloy Produced via Powder Metallurgy Route, Journal of Engineering, Materials and Technology, vol 144 (3), pp. 041009, (2022).

[21] C. M. Wayman, K. Shimizu, The Shape Memory (‘Marmem’) Effect in Alloys, Metal Science Journal, vol 6(1), pp.175-183 (1972).